Evolution effects on parton energy loss with detailed balance

Luan Cheng[1,2,3] and Enke Wang[1,2]

[1]*Institute of Particle Physics, Huazhong Normal University, Wuhan 430079, China*
[2]*Key Laboratory of Quark and Lepton Physics (Huzhong Normal University), Ministry of Education, China*
[3]*Institut für Theoretische Physik, Goethe Universität, Max-von-Laue Strasse 1, D-60438 Frankfurt am Main, Germany*

The initial conditions in the chemically nonequilibrated medium and Bjorken expanding medium at Relativistic Heavy Ion Collider (RHIC) are determined. With a set of rate equations describing the chemical equilibration of quarks and gluons based on perturbative QCD, we investigate the consequence for parton evolution at RHIC. With considering parton evolution, it is shown that the Debye screening mass and the inverse mean free-path of gluons reduce with increasing proper time in the QGP medium. The parton evolution affects the parton energy loss with detailed balance, both parton energy loss from stimulated emission in the chemically nonequilibrated expanding medium and in Bjorken expanding medium are linear dependent on the propagating distance rather than square dependent in the static medium. The energy absorption cannot be neglected at intermediate jet energies and small propagating distance of the energetic parton in contrast with that it is important only at intermediate jet energy in the static medium. This will increase the energy and propagating distance dependence of the parton energy loss and will affect the shape of suppression of moderately high P_T hadron spectra.

I. INTRODUCTION

One of the challenging goals of heavy-ion physics is to detect quark-gluon plasma (QGP). The two nuclei pass through each other, interact, and then produce a dense plasma of quarks and gluons. As the initial parton density is large and the partons suffer many collisions in a very short time, the initial partonic system may attain kinetic equilibrium. But does it attain chemical equilibrium? This question has been investigated in the framework of parton cascade model [1], which is based on the concept of inside-outside cascade [2–4] and evolve parton distributions by a Monte Carlo simulation of a relativistic transport equation involving lowest order perturbative QCD scattering and parton fragmentations. From the numerical studies [5–10] three distinct phases of parton evolution can be distinguished: (1) Gluon thermalize very rapidly, reach approximately isotropic momentum space distribution after a time of the order of 0.3 fm/c. (2) Full equilibration of gluon phase space density takes considerably longer. (3) The evolution of quark distributions lags behind that of the gluons because the relevant QCD cross sections is suppressed by a factor of 2–3. This calculation indicates that the QGP likely to be formed in such collisions are far from chemical equilibrium.

Gluon radiation induced by multiple scattering for an energetic parton propagating in a dense medium leads to induced parton energy loss or jet quenching. Jet quenching is manifested in both the suppression of single inclusive hadron spectra at high transverse momentum p_T region [11] and the disappearance of the typical back-to-back jet structure in dihadron correlation as discovered in high-energy heavy-ion collisions at Relativistic Heavy Ion Collider (RHIC) [12]. The theoretical investigation of jet quenching has been widely carried out in recent years [13–18]. It is found that in the static medium the radiative energy loss is proportional to square of propagating distance. Later the detailed balance effect with gluon absorption was included. It has been shown that the

gluon absorption play an important role for intermediate jet energy region in the static medium [19]. But the plasma is not static, it will expand, cool and become more dilute. Recently medium expansion is included in the jet energy loss by stimulated emission in Ref. [20]. However, only the gluon distribution evolution in a thermodynamical equilibrated expanding medium is considered, the temperature evolution, which plays an important role for Debye screened mass calculation and affects the mean free path and opacity, was neglected in Ref. [20]. Moreover, since the QGP is like to be far from chemical equilibrium, the effect of chemical equilibration on jet energy loss need to be studied.

In this paper, we will study the effects of temperature and fugacity (chemical potential) evolution on jet quenching with detailed balance. In general, the question of thermodynamical equilibration can be decided with microscopic transport models [5]. In this paper, we study a simpler problem which allows us to use a macroscopic model to get the initial conditions and parton evolution. Our strategy will be to assume that the parton distribution can be approximately by thermal phase space distribution with nonequilibrium fugacity λ_g and λ_q of gluon and quark, use a set of rate equations to describe the chemical equilibration of partons, compare dE_T/dy and dN/dy which we get with the data from RHIC, we can then determine the initial conditions of proper time, fugacity, and the time dependence of the parameters T, λ_g and λ_q. We will also study the a thermally-equilibrated and chemically-equilibrated medium expansion—Bjorken expansion with $\lambda_{g(q)} = 1$ and compare the difference. With these results, we obtain the Debye screening mass, mean free path, and opacity from the perturbative QCD at finite temperature in a thermally equilibrated, but chemically nonequilibrated medium and find that they are different with those in thermodynamical medium and static medium. Then, we will investigate the evolution effects on both the final-state radiation associated with the

014901-1

hard processes and the radiation induced by final-state multiple scattering in the medium.

II. PARTON EQUILIBRATION AT RHIC

A. Basic equations

We consider here a thermally equilibrated, but chemically nonequilibrated system, and assume that the parton distribution can be approximated by thermal phase space distributions with nonequilibrium fugacities λ_i which gives the measure of derivation from chemical equilibrium,

$$f(k; T, \lambda_i) = \lambda_i (e^{\beta u \cdot k} \pm \lambda_i)^{-1}, \qquad (1)$$

where β is the inverse temperature and u is the four-velocity of the local moving reference frame, $i = g, q, \bar{q}$ for gluon, quark, antiquark, respectively.

As discussed in Ref. [6], as an approximation the momentum distributions can be written in the factorized Bose or Fermi-Dirac form

$$f(k; T, \lambda_i) = \lambda_i (e^{\beta u \cdot k} \pm 1)^{-1}, \qquad (2)$$

which we will adopt in most of the following calculation.

In general, chemical reactions among partons can be quite complicated because of the possibility of initial and final-state gluon radiations. However, since interference effects due to multiple scatterings inside a dense medium lead to a strong suppression of soft gluon radiation, we shall only consider processes in which a single addition gluon is radiated, such as $gg \rightarrow ggg$. But in order to permit approach to chemical equilibrium, we should also consider the reverse process. Closer inspection shows that gluon radiation is dominated by the process $gg \rightarrow ggg$, because radiative processes involving quarks have substantially smaller cross sections in pQCD, and quarks are considerably less abundant than gluons in the initial phase of the chemical evolution of the parton gas. Here we are interested in understanding the basic mechanisms, so we restrict our consideration to the dominant reaction mechanisms for the equilibration of each parton flavor. These are four processes [6]:

$$gg \leftrightarrow ggg, \quad gg \leftrightarrow q\bar{q}. \qquad (3)$$

Restricting to reactions, the evolution of the parton densities is governed by the master equations,

$$\partial_\mu(\rho_g u^\mu) = \rho_g R_3 (1 - \lambda_g) - 2\rho_g R_2 \left(1 - \frac{\lambda_q \lambda_{\bar{q}}}{\lambda_g^2}\right), \qquad (4)$$

$$\partial_\mu(\rho_q u^\mu) = \rho_q R_2 \left(1 - \frac{\lambda_q \lambda_{\bar{q}}}{\lambda_g^2}\right), \qquad (5)$$

where $R_2 = \frac{1}{2}\sigma_2 n_g$, $R_3 = \frac{1}{2}\sigma_3 n_g$, σ_2 and σ_3 are thermally averaged velocity weighted cross sections, $\sigma_2 = \langle \sigma(gg \rightarrow q\bar{q})v\rangle$ and $\sigma_3 = \langle \sigma(gg \rightarrow ggg)v\rangle$. It has been calculated that $R_2 \approx 0.064 N_f \alpha_s^2 \lambda_g T \ln(7.5/\lambda_g)^2$ and $R_3 = 2.1\alpha_s^2 T(2\lambda_g - \lambda_g^2)^{1/2}$ in Refs. [6,21].

Using Bose and Fermi-Dirac momentum distributions, the gluon and quark densities are related to temperature as

$$\rho_g = \frac{16}{\pi^2}\zeta(3)\lambda_g T^3, \qquad (6)$$

$$\rho_q = \frac{9}{2\pi^2}\zeta(3)N_f \lambda_q T^3, \qquad (7)$$

where $\zeta(3) \approx 1.2$, N_f is the number of dynamical quark flavors.

If we assume that parton scatterings are sufficiently rapid to maintain local thermal equilibrium, and therefore we can neglect effects of viscosity due to elastic and inelastic scatterings, we can have the hydrodynamic equation,

$$\partial_\mu(\varepsilon u^\mu) + P\partial_\mu u^\mu = 0, \qquad (8)$$

where ε and P are energy density and pressure of the hot medium.

In order to obtain analytical solutions, we will neglect the transverse expansion and consider only a purely longitudinal expansion of the parton plasma, so Eq. (8) can be rewritten as

$$\frac{d\varepsilon}{d\tau} + \frac{\varepsilon + P}{\tau} = 0. \qquad (9)$$

With the additional constraint of the baryon number conservation, we get

$$\partial_\mu(\rho_B u^\mu) = 0. \qquad (10)$$

Once the initial conditions are obtained, the evolution of temperature $T(\tau)$, and fugacity $\lambda_g(\tau)$, $\lambda_q(\tau)$ can be determined by solving the rate Eqs. (4), (5), (9), and (10) together. So the input of the initial condition plays an important role to investigate the effects of the evolution for the parton system.

B. Initial conditions

1. Transverse energy

In order to solve the rate equations discussed in the last section, one has to specify the initial conditions.

The transverse energy per unit rapidity can be expressed as [22]

$$\frac{dE_T}{dy} = \tau A \int d\eta d^2 p_T p_T^2 \cosh\xi f(k; T, \lambda_i), \qquad (11)$$

where $\xi = y - \eta$, y, and η are the rapidity and pseudorapidity, respectively.

Using the momentum distribution discussed in last section, the transverse energy per unit rapidity can be deduced as

$$\frac{dE_T}{dy} = [g_f(\lambda_q + \lambda_{\bar{q}}) + g_b\lambda_g]\frac{\tau\pi R^2}{2\pi^3}\int d\eta d^2 p_T p_T^2$$
$$\times \cosh\xi e^{-\frac{p_T \cosh\xi}{T(\tau)}}. \qquad (12)$$

For the antiquark fugacity, $\lambda_{\bar{i}} = \lambda_i^{-1}$. We take $\tau_0 = 0.3$ fm as in Ref. [6]. The QGP medium freezes out when the temperature reduces to about 160–170 MeV. With different initial temperature T_0, we will get different parton equilibration and then different curves of transverse energy per unit rapidity dE_T/dy as the function of λ_{g0} at the freezing out time (4.4 fm) as shown in Fig. 1.

The data from RHIC show that at $\sqrt{s} = 200A$ GeV transverse energy per unit rapidity is $dE_T/dy|_{y=0} = 620 \pm 33$ GeV [23] for the 5% most central events of Au-Au collisions. It is found that curve of the transverse energy per unit rapidity does not intersect the straight line $dE_T/dy|_{y=0} = 620$ GeV if
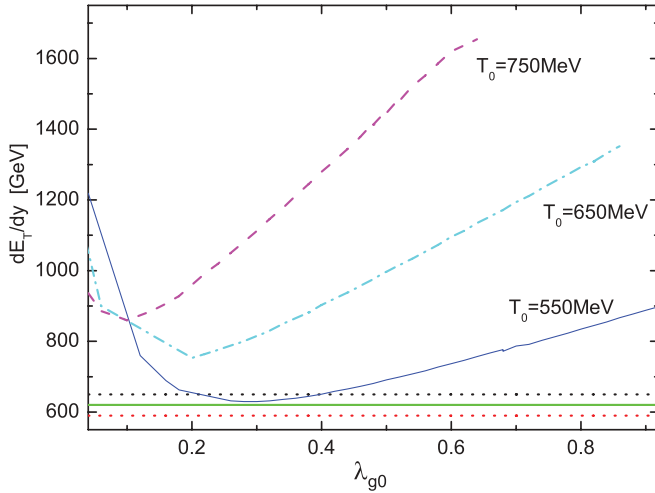
FIG. 1. (Color online) The initial fugacity λ_{g0} dependence of transverse energy per unit rapidity for the most central events. The solid, dash-dot, and dash curves show the results of dE_T/dy for initial proper time $\tau_0 = 0.3$ fm and initial temperature $T_0 = 550$ MeV, 650 MeV, 750 MeV at the freezing out time, respectively. The area between the two dot line is the data $dE_T/dy|_{y=0} = 620 \pm 33$ GeV for the 5% most central events of Au-Au collisions from RHIC [23].

the initial temperature is higher than 550 MeV, only when the initial temperature is $T_0 = 550$ MeV, $\lambda_{g0} = 0.3$, the curve is tangential to the straight line. $dE_T/dy|_{y=0} = 620 \pm 33$ GeV [23] for the 5% most central events of Au-Au collisions is measured after the time freeze-out. After freezing out hard scattering seldom happens so that there is little transverse momentum transfer and $dE_T/dy|_{y=0}$ is stable. Here only tangential point is the minimum of the curve and stable. If the initial temperature is lower than 550 MeV they have two points of intersection, which, however, are not stable. It implies that the initial temperature is 550 MeV, λ_{g0} is 0.3 for the central events of Au-Au collisions at RHIC. We obtain the initial temperature of 420 MeV when fitting $dE_T/dy|_{y=0}$ with $\lambda_{g(q)} = 1$ under the Bjorken expansion condition ($T^3\tau = T_0^3\tau_0$).

2. Particle multiplicities

Secondly we demonstrate that the initial condition determined above is consistent with that from the particle multiplicities.

The thermodynamic functions for a many-particle system for an ensemble at temperature T and fugacity λ can be derived from the grand partition,

$$lnZ_F = \frac{g_F V}{6\pi^2 T} \int_0^\infty dp \frac{p^4}{(p^2 - m^2)^{1/2}} \left[\frac{1}{1 + \lambda^{-1}e^{\beta\sqrt{p^2+m^2}}} \right.$$
$$\left. + \frac{1}{1 + \lambda e^{\beta\sqrt{p^2+m^2}}} \right] \qquad (13)$$

for fermions and

$$lnZ_B = \frac{g_B V}{6\pi^2 T} \int_0^\infty dp \frac{p^4}{(p^2 - m^2)^{1/2}} \frac{1}{\lambda^{-1}e^{\beta\sqrt{p^2+m^2}} - 1} \qquad (14)$$

for bosons, where g_F and g_B are the degeneracy factors of fermions and bosons, V is the volume of the parton gas.

If we neglect the mass for light quarks and gluons, the momentum integral Eqs. (13), (14) can be calculated exactly. For light quarks and gluon the grand partition functions can be expressed as

$$TlnZ_{q(\bar{q})} = \frac{g_q V}{\pi^2}(\lambda_q + \lambda_q^{-1})T^4, \qquad (15)$$

$$TlnZ_g = \frac{g_g V}{\pi^2}\lambda_g T^4. \qquad (16)$$

In order to get the expressions for the entropy density and particle number density, we recall the first law of thermodynamics

$$E = F(V, T, \mu) + TS(V, T, \mu) + \mu N(V, T, \mu), \qquad (17)$$

where F, T, S, μ, N are the free energy, temperature, entropy, chemical potential and particle number, respectively.

We can evaluate the free energy and the average value of particle number for the grand-canonical partition function. With the thermodynamics Eq. (17), we obtain the entropy density in the chemically nonequilibrated medium as

$$s = \frac{48}{\pi^2}(\lambda_q + \lambda_q^{-1})T^3 + \frac{64}{\pi^2}\lambda_g T^3$$
$$- ln\lambda_q(\lambda_q - \lambda_q^{-1})\frac{12}{\pi^2}T^3 - (ln\lambda_g)\lambda_g\frac{16}{\pi^2}T^3. \qquad (18)$$

In hydrodynamics, the relation between entropy S and particle number N is $S/N = 4$. In a thermally equilibrated but chemically nonequilibrated system here, with considering the thermodynamics Eq. (17) and the grand canonical partition functions Eqs. (15) and (16), we can deduce

$$\frac{S}{N} = \frac{E + PV - \mu N}{TN} = \frac{s_i}{dN_i/dy/\tau\pi R^2} = 4 - ln\lambda_i, \quad (19)$$

where s_i and dN_i/dy are the entropy density and particle number distribution for quarks, antiquarks, and gluons.

So we have

$$dN/dy = \sum_i dN_i/dy$$
$$= \frac{\tau\pi R^2}{4 - ln(\lambda_q)}\left[\frac{48}{\pi^2}\lambda_q T^3 - (ln\lambda_q)\lambda_q\frac{12}{\pi^2}T^3\right]$$
$$+ \frac{\tau\pi R^2}{4 - ln(\lambda_q^{-1})}\left[\frac{48}{\pi^2}\lambda_q^{-1}T^3 - (ln\lambda_q^{-1})\lambda_q^{-1}\frac{12}{\pi^2}T^3\right]$$
$$+ \frac{\tau\pi R^2}{4 - ln(\lambda_g)}\left[\frac{64}{\pi^2}\lambda_g T^3 - (ln\lambda_g)\lambda_g\frac{16}{\pi^2}T^3\right], \qquad (20)$$

where R is the transverse radius of the medium and taken as 6.5 fm, which is approximately the size of radius of Au nucleus.

As discussed in the above subsection, with different initial conditions T_0, λ_{g0}, and λ_{q0}, we obtain the different particle multiplicities dN/dy as shown in Fig. 2. The data from RHIC shows that particle multiplicities $dN/dy = 1500$ at $\sqrt{s} = 200A$ GeV from Ref. [20]. Comparing our calculations
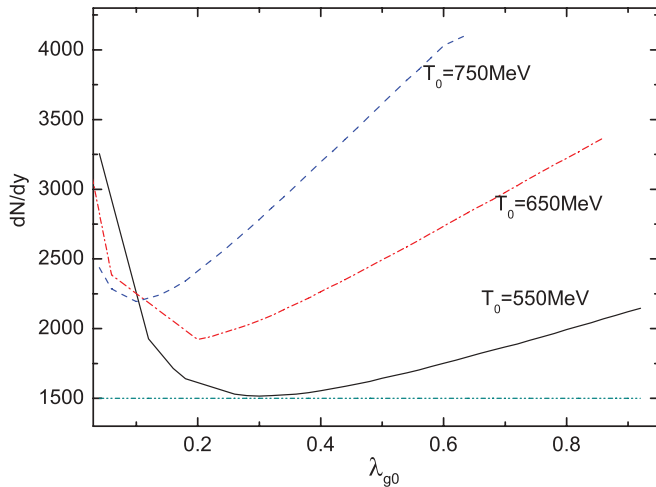
FIG. 2. (Color online) The initial fugacity λ_{g0} dependence of particle multiplicities. The solid, dash-dot, and dash curves show the results for initial proper time $\tau_0 = 0.3$ fm and initial temperature $T_0 = 550$ MeV, 650 MeV, 750 MeV, respectively. The dot line indicate $dN/dy = 1500$ from Ref. [20].

with the data from RHIC, we can conclude that the initial conditions which we obtain here are consistent with that from transverse energy.

C. Parton equilibration

With the initial conditions obtained above and rate Eqs. (4), (5), energy conservation Eq. (9), and baryon number conservation Eq. (10), we can obtain the parton evolution in a chemically nonequilibrated system. The evolution of temperature and fugacity is shown in Figs. 3 and 4. We find that the parton gas cools faster than predicted in Bjorken expanding medium ($\lambda_{g(q)} = 1$) as shown in Fig. 3 because the production of additional partons approaching the chemical equilibrium state consumes an appreciable amount of energy. Figure 4 shows that fugacity of gluons λ_g and quarks λ_q increase with
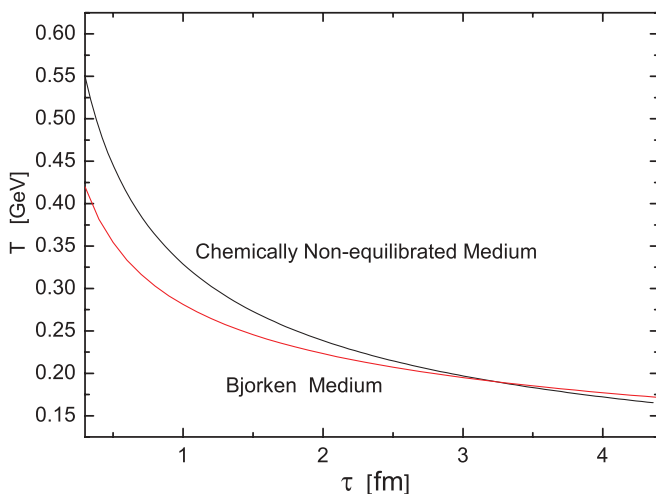

FIG. 3. (Color online) Time evolution of the temperature T in chemically nonequilibrated medium and in Bjorken expanding medium in Au + Au collisions for 200 GeV/nucleon at RHIC.
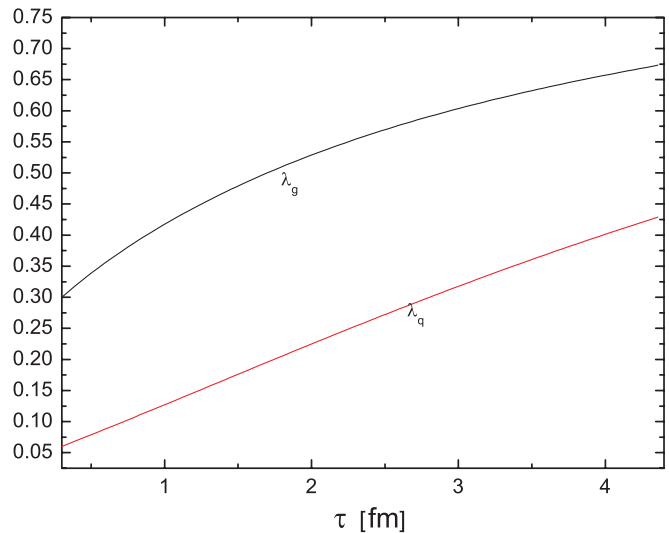

FIG. 4. (Color online) Time evolution of the fugacities λ_g and λ_q of gluons and quarks in the Au + Au collisions for 200 GeV/nucleon at RHIC.

increasing the proper time τ, until the medium freezes out it has not been totally chemically equilibrated.

III. OPACITY IN A CHEMICAL NONEQUILIBRATED QGP MEDIUM

Parton evolution will lead to the evolution of the Debye screening mass and parton number density. It will affect the cross section between the jet and the medium partons, and the opacity when the jet propagates through the QGP medium.

The Debye screening mass μ_D is generated by medium effects [24]. Using Bose and Fermi equilibrium distributions in the above section, one gives the Debye screening mass,

$$\mu_D^2 = \frac{6g^2}{\pi^2} \int_0^\infty k f(k) dk \qquad (21)$$

$$= \frac{4}{3} \pi \alpha_s T^2 (\lambda_q + 2\lambda_g). \qquad (22)$$

Using the parton evolution in the above section, we can obtain how μ_D^2 evolves with the proper time in a chemically nonequilibrated QGP medium and in Bjorken expanding medium ($\lambda_{g(q)} = 1$) as shown in Fig. 5. We can see that the Debye screening mass in the chemically nonequilibrated medium is less than that in the Bjorken expanding medium ($\lambda_{g(q)} = 1$) because of the less fugacity in the chemically nonequilibrated medium.

The cross sections for the processes, such as $gg \to gg$ and $gq \to gq$, can be calculated from the pQCD, the leading order elastic scattering cross sections can be expressed as

$$\sigma_{gg} \simeq \frac{9\pi \alpha_s^2}{2\mu_D^2}, \quad \sigma_{gq} \simeq \frac{2\pi \alpha_s^2}{\mu_D^2}, \qquad (23)$$

where μ_D is the Debye screening mass generated from the medium effects with considering both quark and gluon contributions [19].
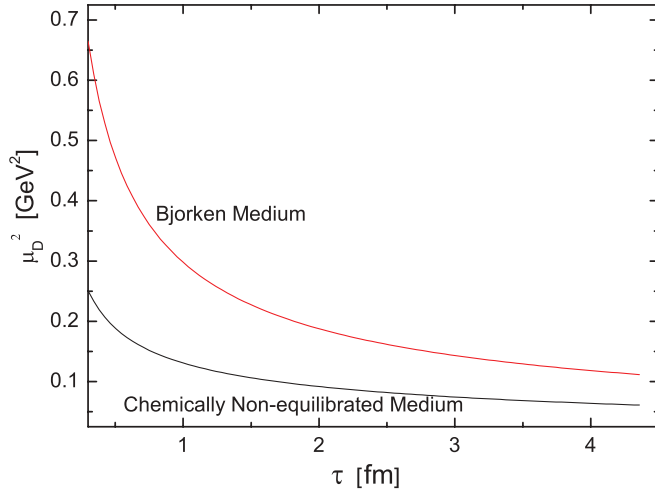
FIG. 5. (Color online) Time evolution of the Debye screening mass in chemically nonequilibrated medium and in Bjorken expanding medium in the Au + Au collisions for 200 GeV/nucleon at RHIC.

Hence, the inverse mean free path for a gluon l_g is [25]

$$
\begin{aligned}
l_g^{-1} &= \sigma_{gg}\rho_g + \sigma_{gq}\rho_q \\
&\simeq \frac{72\alpha_s^2}{\mu_D^2\pi}\zeta(3)\lambda_g T^3 + \frac{9\alpha_s^2}{\mu_D^2\pi}\zeta(3)N_f\lambda_q T^3.
\end{aligned}
\tag{24}
$$

From the above results in the last section of parton equilibration, one can obtain the proper time dependence of the inverse mean free path as shown in Fig. 6, the inverse mean free path decreases with increasing proper time, the inverse mean free path in the chemically nonequilibrated medium is larger than that in Bjorken expanding medium ($\lambda_{g(q)} = 1$) due to less Debye screening mass and larger temperature in the chemically nonequilibrated medium.

We assume that jet travel the distance of L at speed of light in the chemically nonequilibrated QGP medium. The opacity, the mean number of collisions in the medium, can be written
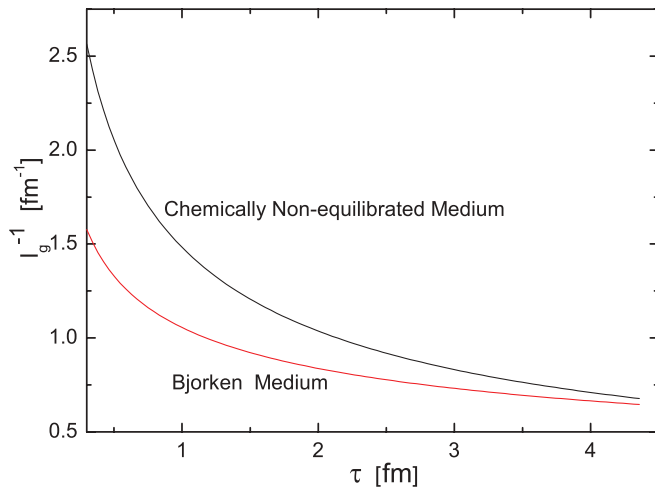

FIG. 6. (Color online) Time evolution of the inverse mean free-path for gluon in chemically nonequilibrated medium and in Bjorken expanding medium in the Au + Au collisions for 200 GeV/nucleon at RHIC.
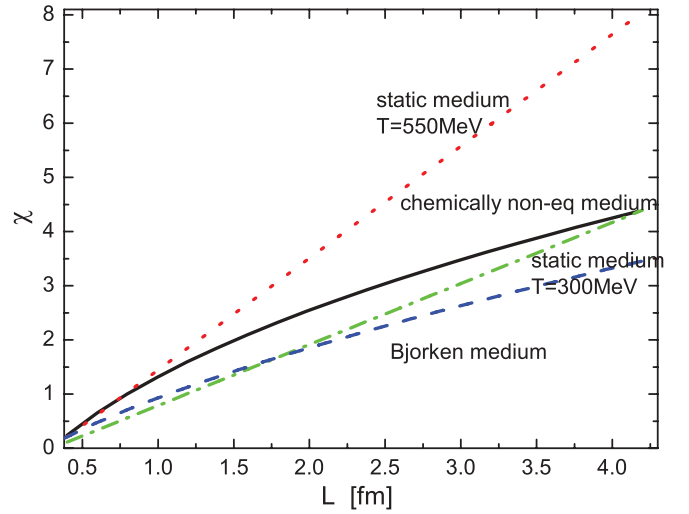

FIG. 7. (Color online) Propagating distance dependence of the opacity in the Au + Au collisions for 200 GeV/nucleon at RHIC. The dotted curve is the opacity in a static medium for temperature $T = 550$ MeV, and the dotted dash curve is the opacity in a static medium at temperature $T = 300$ MeV. The solid and dash curve indicate that in the chemically nonequilibrated expanding medium for $T_0 = 550$ MeV and the Bjorken expanding medium for $T_0 = 420$ MeV, respectively.

as the integration of collision number l_g^{-1} per unit length,

$$
\chi = \int_{\tau_0}^{\tau_0+L} (\sigma_{gg}\rho_g + \sigma_{gq}\rho_q)d\tau.
\tag{25}
$$

Using the result from parton equilibration in above section, the propagating distance L dependence of the opacity is shown in Fig. 7. We can see that the opacity increases with increasing the propagating distance L. The opacity at the initial temperature $T = 550$ MeV in the static medium, which means that the medium always stay at the initial temperature, is larger than that in the chemically nonequilibrated and Bjorken expanding medium ($\lambda_{g(q)} = 1$) because of the decrease of the temperature and density in the expanding medium. In the chemically nonequilibrated expanding QGP medium, the opacity is larger than that in Bjorken expanding medium because of the higher temperature and the different ratio of quarks and gluons in the two mediums. One also finds that the opacity in the chemically nonequilibrated medium with the initial temperature $T = 550$ MeV is larger than that in a static medium at the temperature $T = 300$ MeV as considered in Ref. [16].

IV. PARTON ENERGY LOSS WITH DETAILED BALANCE

The theoretical investigation of jet quenching are mostly carried out in a static medium and is found that the radiative energy loss is proportional to the square of propagating distance because of non-Abelian effect. However, the QGP medium is an expanding medium with evolution instead of being static. In this section, we will compare the difference of propagating distance L dependence in the different medium

and the ratio of effective parton energy loss with and without absorption to study the evolution effects on jet quenching.

In the leading-log approximation in an axial gauge the final-state radiation amplitude of a quark can be factorized from the hard scattering. Taking into account both stimulated emission and thermal absorption in the chemically nonequilibrated expanding hot medium, one obtains the probability of gluon radiation with energy ω to the zeroth order opacity (self-quenching and absorption) [19]

$$
\frac{dP^{(0)}}{d\omega} = \frac{\alpha_s C_F}{2\pi} \int \frac{dz}{z} \int \frac{dk_\perp^2}{k_\perp^2} [f_g(zE)\delta(\omega + zE)
$$
$$
+ (1 + f_g(zE))\delta(\omega - zE)\theta(1 - z)]P_{gq}\left(\frac{\omega}{E}\right), \quad (26)
$$

where C_F is the Casimir of the quark jet, $f_g(k)$ is the gluon distribution which has been shown in Eq. (2), and the splitting function $P_{gq}(z) \equiv P(z)/z = [1 + (1 - z)^2]/z$ for $q \to gq$. The first term corresponds to thermal absorption and the second term corresponds to gluon emission with the Bose-Einstein enhancement factor.

Assuming the scale of the hard scattering to be $Q^2 = 4E^2$ and considering gluon radiation outside a cone with $|k_\perp| > \mu_D$, one has the kinematic limits of the gluon's transverse momentum [19],

$$
\mu_D^2 \leqslant k_{\perp\max}^2 \leqslant 4|\omega|(E - \omega). \quad (27)
$$

Subtracting the gluon radiation spectrum in the vacuum ($T = 0$), one then obtains the energy loss due to final absorption and stimulated emission when the jet passes through the chemically nonequilibrated hot medium over the distance L,

$$
\Delta E_{abs}^{(0)} = \frac{L}{L_0} \int d\omega\, \omega \left(\frac{dP^{(0)}}{d\omega} - \frac{dP^{(0)}}{d\omega}\bigg|_{T=0} \right)
$$
$$
= \frac{\alpha_s C_F L}{2\pi L_0} \int dz \int \frac{dk_\perp^2}{k_\perp^2} [-P(-z)f_g(zE)
$$
$$
+ P(z)f_g(zE)\theta(1 - z)]
$$
$$
= -\frac{\pi \alpha_s C_F L \langle T \rangle^2}{3 L_0 E} \left[\ln \frac{4E\langle T \rangle}{\mu_D^2} + 2 - \gamma_E + \frac{\zeta'(2)}{\pi^2} \right], \quad (28)
$$

where $\gamma_E \approx 0.5772$, $\zeta'(2) \approx -0.9376$, L_0 is the thickness of the QGP medium, which we estimate as the diameter of the Au nucleus, and $\langle T \rangle$ is the average temperature during the time the jet propagates through the medium,

$$
\langle T \rangle = \frac{1}{L} \int_{\tau_0}^{L} T(\tau)d\tau. \quad (29)
$$

As shown in Fig. 8, we see that the energy loss without rescattering increases with increasing L at fixed $E = 5$ GeV, the energy gain without rescattering in the chemically nonequilibrated expanding medium is larger than that in the Bjorken expanding medium ($\lambda_{g(q)} = 1$) because of the higher temperature in the chemically nonequilibrated medium.

During the propagation of the jet after its production, it will suffer multiple scattering with targets in the medium. It was shown that the higher order opacity corrections contribute little to the radiative energy loss [16], so we will focus on
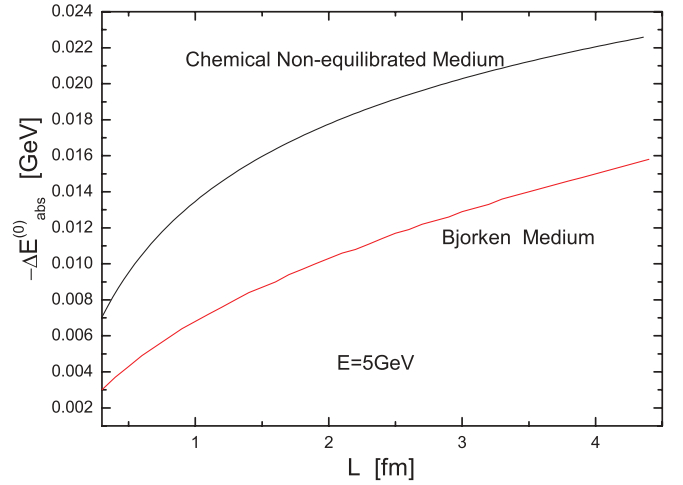

FIG. 8. (Color online) Propagating distance dependence of the energy gain without rescattering in chemically nonequilibrated medium and in Bjorken expanding medium.

the stimulated emission and thermal absorption associated with rescattering with considering parton equilibration in a chemically nonequilibrated hot medium. We use the model which is initially proposed by Gyulassy-Wang (GW) to describe the interaction between the jet and target partons by a static color-screened Yukawa potential [25]. Assuming that a parton is produced at $\mathbf{y}_0 = (y_0, \mathbf{y}_{0\perp})$ inside the medium with y_0 being the longitudinal coordinate, the Yukawa potential is

$$
V_n = 2\pi \delta(q^0) v(q_n) e^{-i q_n \cdot y_n} t_{a_n}(j) t_{a_n}(n), \quad (30)
$$
$$
v(q_n) = \frac{4\pi \alpha_s}{q_n^2 + \mu_D^2}, \quad (31)
$$

where q_n is the momentum transfer from a target parton n at the position $\mathbf{y}_n = (y_n, \mathbf{y}_{n\perp})$, $t_{a_n}(j)$ and $t_{a_n}(n)$ are the color matrices for the jet and target parton.

Here we consider the contributions to the first order in the opacity expansion. By including the interference between the process of the rescattering and non-rescattering, we obtain the energy loss for stimulated emission $\Delta E_{rad}^{(1)}$ and energy gain for thermal absorption $\Delta E_{abs}^{(1)}$ to the first order as

$$
\Delta E_{rad}^{(1)} = \frac{\alpha_s C_F E}{\pi} \int_{\tau_0}^{\tau_0 + L} d\tau \int dz \int \frac{dk_\perp^2}{k_\perp^2} \int d^2 q_\perp
$$
$$
\times |\bar{v}(q_\perp)|^2 \frac{k_\perp \cdot q_\perp}{(k_\perp - q_\perp)^2} P(z)(\sigma_{gg}\rho_g + \sigma_{gq}\rho_q)
$$
$$
\times \langle \text{Re}(1 - e^{i\omega_1 y_{10}}) \rangle \theta(1 - z), \quad (32)
$$
$$
\Delta E_{abs}^{(1)} = \frac{\alpha_s C_F E}{\pi} \int_{\tau_0}^{\tau_0 + L} d\tau \int dz \int \frac{dk_\perp^2}{k_\perp^2} \int d^2 q_\perp
$$
$$
\times |\bar{v}(q_\perp)|^2 \frac{k_\perp \cdot q_\perp}{(k_\perp - q_\perp)^2} f_g(zE)(\sigma_{gg}\rho_g + \sigma_{gq}\rho_q)
$$
$$
\times [-P(-z)\langle \text{Re}(1 - e^{i\omega_1 y_{10}}) \rangle
$$
$$
+ P(z)\langle \text{Re}(1 - e^{i\omega_1 y_{10}}) \rangle \theta(1 - z)], \quad (33)
$$

where $\omega_1 = (k_\perp - q_\perp)^2/2\omega$, the factor $(1 - e^{i\omega_1 y_{10}})$ reflects the destructive interference arising from the non-Abelian LPM effect. Averaging over the longitudinal target profile
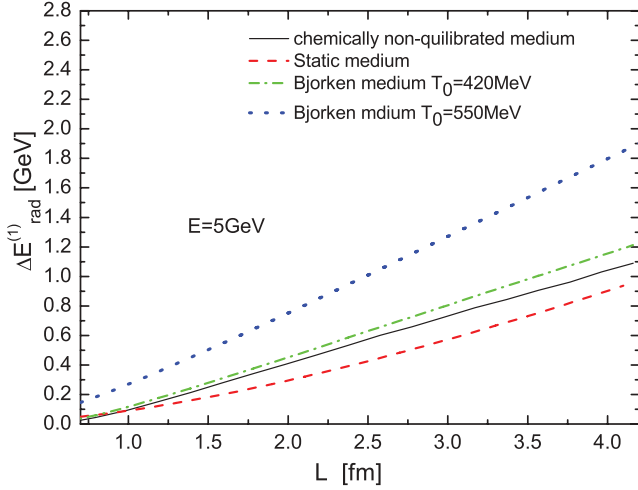
FIG. 9. (Color online) Propagating distance dependence of the energy loss to the first order opacity. For static medium case, $T = 300 \, \text{MeV}$, $\mu_D = 0.5 \, \text{GeV}$, and $l_g = 1 \, \text{fm}$ [16]. For the chemically nonequilibrate medium case, $T_0 = 550 \, \text{MeV}$, $\lambda_{g0} = 0.3$, and $\tau_0 = 0.3 \, \text{fm}$. For the Bjorken expanding case with two different initial temperature, $T_0 = 420 \, \text{MeV}$ and $T_0 = 550 \, \text{MeV}$, $\tau_0 = 0.3 \, \text{fm}$.

FIG. 10. (Color online) Propagating distance dependence of the energy gain to the first order. For static medium case, $T = 300 \, \text{MeV}$, $\mu_D = 0.5 \, \text{GeV}$, and $l_g = 1 \, \text{fm}$ [16]. For the chemically nonequilibrate medium case, $T_0 = 550 \, \text{MeV}$, $\lambda_{g0} = 0.3$, and $\tau_0 = 0.3 \, \text{fm}$. For the Bjorken expanding case, $T_0 = 420 \, \text{MeV}$, $\tau_0 = 0.3 \, \text{fm}$.

is defined as $\langle \cdots \rangle = \int dy \rho(y) \cdots$. The target parton number distribution along the jet direction in the QGP medium is assumed to be an exponential form $\rho(y) = 2 \exp(-2y/L)/L$. $|\bar{v}(\mathbf{q}_\perp)|^2$ is the normalized distribution of momentum transfer from the scattering centers,

$$|\bar{v}(\mathbf{q}_\perp)|^2 \equiv \frac{1}{\sigma_{el}} \frac{d^2 \sigma_{el}}{d^2 \mathbf{q}_\perp} = \frac{1}{\pi} \frac{\mu_{\text{eff}}^2}{\left(\mathbf{q}_\perp^2 + \mu_D^2\right)^2}, \quad (34)$$

$$\frac{1}{\mu_{\text{eff}}^2} = \frac{1}{\mu_D^2} - \frac{1}{q_{\perp\text{max}}^2 + \mu_D^2}, q_{\perp\text{max}}^2 \approx 3E\mu_D. \quad (35)$$

The propagating distance dependence of the energy loss and energy gain for stimulated emission and thermal absorption is shown in Figs. 9 and 10 at fixed jet energy $E = 5 \, \text{GeV}$.

In the limit of $EL \gg 1$ and $E \gg \mu_D$, the approximate asymptotic behavior of the energy loss of stimulated emission [16] and energy gain of thermal absorption [19] in a static medium are

$$\frac{\Delta E_{\text{rad}}^{(1)}}{E} \approx \frac{\alpha_s C_F \mu_D^2 L^2}{4 l_g E} \left[ln \frac{2E}{\mu_D^2 L} - 0.048 \right], \quad (36)$$

$$\frac{\Delta E_{\text{abs}}^{(1)}}{E} \approx -\frac{\pi \alpha_s C_F}{3} \frac{L T^2}{l_g E^2} \left[ln \frac{\mu_D^2 L}{T} - 1 + \gamma_E - \frac{6\zeta'(2)}{\pi^2} \right]. \quad (37)$$

As shown in Eq. (36), the analytic approximation of the energy loss by stimulated emission in a static medium is proportional to $L^2 ln(\frac{1}{L})$. We fit the curve from our numerical calculation in a chemically nonequilibrated medium, it is shown as in Fig. 9 that the energy loss by stimulated emission is proportional to L approximately by taking into account the parton evolution of the chemically nonequilibrated medium and Bjorken expanding medium ($\lambda_{g(q)} = 1$). In a static medium
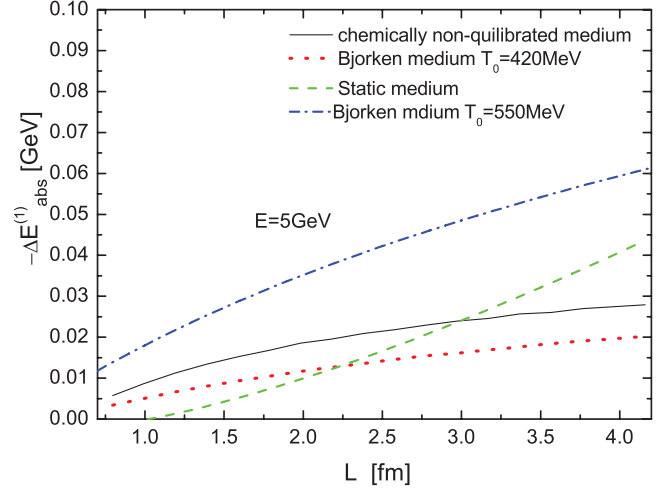
it is shown that the energy gain $\Delta E_{\text{abs}}^{(1)}$ in Eq. (37), from thermal absorption is linear distance dependence if assuming $\mu_D^2 L/T \gg 1$, and become a quadratic distance dependence if assuming $\mu_D^2 L/T \ll 1$. In our case for a chemically nonequilibrated medium here, from the curve fitting it is shown as in Fig. 10 that the energy gain keep the linear distance dependence as $\mu_D^2 L/T \gg 1$, but the distance dependence becomes $L^{0.2}$ as $\mu_D^2 L/T \ll 1$ instead of L^2 dependence in the static medium case and the proportionality factor is much smaller than that in the static medium.

As shown in Fig. 9, the energy loss without thermal absorption in a chemically nonequilibrated medium with initial temperature $T_0 = 550 \, \text{MeV}$, initial fugacity $\lambda_{g0} = 0.3$ is larger than that in a static medium with $T = 300 \, \text{MeV}$, $\mu_D = 0.5 \, \text{GeV}$, and the mean free path of the jet $l_g = 1 \, \text{fm}$ as considered in Ref. [16]. But it is less than that in the Bjorken expanding medium ($\lambda_{g(q)} = 1$) with $T_0 = 420 \, \text{MeV}$. Although the opacity in the Bjorken expanding medium is less than that in the chemically nonequilibrated expanding medium, the Debye screening mass is larger, this leads to larger $q_{\perp\text{max}}$ and larger energy loss per collision. We also calculated the energy loss without thermal absorption in the Bjorken medium ($\lambda_{g(q)} = 1$) with the same initial temperature $T_0 = 550 \, \text{MeV}$ as in chemically nonequilibrated medium to study difference between Bjorken expansion and chemically nonequilibrated expansion medium. It is shown that the energy loss without thermal absorption in the Bjorken medium is larger than that in the chemically nonequilibrated medium due to that temperature decreases more rapidly in the chemically nonequilibrated medium than the Bjorken expanding medium ($\lambda_{g(q)} = 1$). As shown in Fig. 10, the energy gain in the chemically nonequilibrated medium is a bit larger than that in the Bjorken expanding medium ($\lambda_{g(q)} = 1$) with $T_0 = 420 \, \text{MeV}$ due to the larger temperature in the chemically nonequilibrated medium.
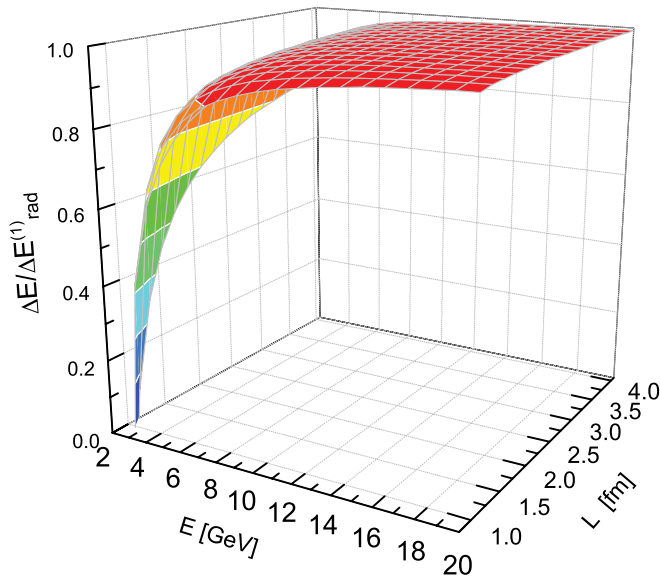
FIG. 11. (Color online) The ratio of effective parton energy loss with and without absorption as a function of parton energy E and propagating distance L.

Figure 11 shows the ratio between parton energy loss $\Delta E = \Delta E_{\rm rad}^{(1)} + \Delta E_{\rm abs}^{(1)} + \Delta E_{\rm abs}^{(0)}$ with thermal absorption and the radiative energy loss $\Delta E_{\rm rad}^{(1)}$ without thermal absorption, which is $\Delta E/\Delta E_{\rm rad}^{(1)} = 1 + (\Delta E_{\rm abs}^{(1)} + \Delta E_{\rm abs}^{(0)})/\Delta E_{\rm rad}^{(1)}$, as functions of parton energy E and propagating distance L in a chemically nonequilibrated medium. The more the ratio is suppressed than unit, the more the energy gain contributes. It is shown that the energy gain via absorption is important for intermediate parton energy and small propagating distance. The absorption can be neglected either for asymptotically large parton energy or large values of L. The comparison between the ratios in a static medium and in a chemically nonequilibrated hot medium at fixed parton energy $E = 3$ GeV is shown in Fig. 12. We can
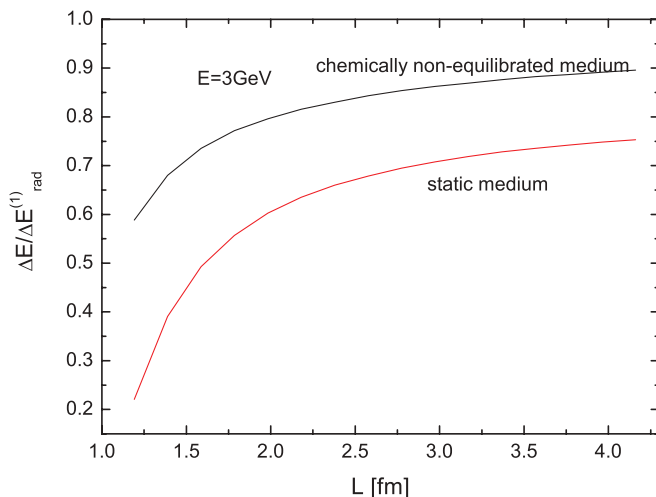

FIG. 12. (Color online) The ratio of effective parton energy loss with and without absorption as a function of propagating distance L at fixed $E = 3$ GeV in a static medium and chemically nonequilibrated hot medium cases.

see that the ratio of the calculated parton energy loss with and without thermal absorption in a static medium ($T = 550$ MeV, $\mu_D = 1$ GeV) considered in Ref. [19] is less than that in a chemically nonequilibrated hot medium. This result implies that the energy gain via absorption is more important in a static medium than that in a chemically nonequilibrated medium at large distance L and intermediate jet energy region.

V. CONCLUSION

In summary, we have determined the initial conditions for central Au-Au collisions at RHIC. It is shown that the initial temperature is 550 MeV, the initial fugacity λ_g for gluons is 0.3 and λ_q for quarks is 0.06 for the chemically nonequilibrated expanding medium. The initial temperature is 420 MeV for the Bjorken expanding medium. We obtain that partons cool faster than predicted by Bjorken with the proper time. This chemical equilibration in a hot medium lead to that the Debye mass and the inverse mean free-path decrease with increasing the proper time, and the opacity for a energetic parton in a chemically nonequilibrated medium increases with increasing the propagating distance L. The Debye mass and the mean free-path in the Bjorken expanding medium is larger than that in the chemically nonequilibrated expanding medium. We found that the opacity in the chemically nonequilibrated medium is larger than that in the static medium at temperature 300 MeV and that in the Bjorken expanding medium, but is less than that in a static medium at $T = 550$ MeV.

The parton evolution affect the energy loss with detailed balance. The propagating distance L dependence of parton energy loss with detailed balance is determined. The net effect of stimulated gluon emission and thermal absorption are considered for an energetic parton propagating inside the QGP medium. It is shown that, by taking into account the evolution of the temperature and fugacity, the energy loss from stimulated emission is proportional to L in the chemically nonequilibrated medium and Bjorken expanding medium rather than L^2 dependence on the propagating distance in the static medium. The energy loss in the chemically nonequilibrated medium is a bit less than that in Bjorken expanding medium. Because of the higher temperature in the chemically nonequilibrated medium, the energy gain without rescattering to the first order opacity in the chemically nonequilibrated medium are larger than those in the Bjorken medium. The relative reduction of the parton energy loss is significant at intermediate parton energy E and small propagating distance L in the chemically nonequilibrium medium. The evolution of the medium modifies the jet energy loss in the intermediate energy region and affect the shape of suppression intermediate high P_T hadrons spectrum.

[1] K. Geiger and B. Muller, Nucl. Phys. B **369**, 600 (1992); K. Geiger, Phys. Rep. **258**, 237 (1995).

[2] R. Anishetty, P. Koehler, and L. McLerran, Phys. Rev. D **22**, 2793 (1980).

[3] R. C. Hwa and K. Kajantie, Phys. Rev. Lett. **56**, 696 (1986).

[4] J. P. Balizt and A. H. Mueller, Nucl. Phys. B **289**, 847 (1987).

[5] K. Geiger and J. I. Kapusta, Phys. Rev. D **47**, 4905 (1993).

[6] T. S. Biró, B. Müller, M. H. Thoma, and X. N. Wang, Nucl. Phys. A **566**, 543c (1994).

[7] K. Geiger, Phys. Rev. D **46**, 4965 (1992); **46**, 4986 (1992).

[8] I. Kawrakow, H. J. Mohring, and J. Ranft, Nucl. Phys. A **544**, 471c (1992).

[9] E. Shuryak, Phys. Rev. Lett. **68**, 3270 (1992).

[10] B. Muller and X. N. Wang, Phys. Rev. Lett. **68**, 2437 (1992).

[11] K. Adcox *et al.*, Phys. Rev. Lett. **88**, 022301 (2001); C. Adler *et al.*, *ibid.* **89**, 202301 (2002).

[12] C. Adler *et al.*, Phys. Rev. Lett. **90**, 082302 (2003).

[13] M. Gyulassy and X.-N. Wang, Nucl. Phys. B **420**, 583 (1994); X.-N. Wang, M. Gyulassy, and M. Plumer, Phys. Rev. D **51**, 3436 (1995).

[14] R. Baier, Y. L. Dokshitzer, S. Peigne, and D. Schiff, Phys. Lett. B **345**, 277 (1995); R. Baier, Y. L. Dokshitzer, A. H. Mueller, S. Peigne, and D. Schiff, Nucl. Phys. B **484**, 265 (1997).

[15] B. G. Zakharov, JETP Lett. **63**, 952 (1996); **65**, 615 (1997).

[16] M. Gyulassy, P. Levai, and I. Vitev, Phys. Rev. Lett. **85**, 5535 (2000); Nucl. Phys. B **594**, 371 (2001); M. Gyulassy, I. Vitev, X. N. Wang, and B. W. Zhang, *Quark Gluon Plasma 3*, edited by R. C. Hwa and X. N. Wang (World Scientific, Singapore, 2003), pp. 123–191.

[17] U. A. Wiedemann, Nucl. Phys. B **588**, 303 (2000).

[18] X. Guo and X.-N. Wang, Phys. Rev. Lett. **85**, 3591 (2000).

[19] E. Wang and X.-N. Wang, Phys. Rev. Lett. **87**, 142301 (2001).

[20] Miklos Gyulassy, Ivan Vitev, Xin-Nian Wang, and Pasi Huovinen, Phys. Lett. B **526**, 301 (2002).

[21] Xin-Nian Wang, Phys. Rep. **280**, 287 (1997).

[22] Z. Xu and C. Greiner, Phys. Rev. C **71**, 064901 (2005).

[23] J. Adams *et al.* (STAR Collaboration), Phys. Rev. C **70**, 054907 (2004).

[24] E. Braaten and R. D. Pisarski, Nucl. Phys. B **337**, 569 (1990).

[25] X.-N. Wang, M. Gyulassy, and M. Plumer, Phys. Rev. D **51**, 3436 (1995).